Nature Environment and Pollution Technology
An International Quarterly Scientific Journal

p-ISSN: 0972-6268
(Print copies up to 2016)
e-ISSN: 2395-3454

Vol. 24 | No. 1 | Article ID B4144 | 2025

Original Research Paper

https://doi.org/10.46488/NEPT.2025.v24i01.B4144

Open Access Journal

Forward Osmosis Process for Concentration of Treated Tannery Effluent

S. U. Sayyad[1,2†]

[1]Department of Civil Engineering, Indian Institute of Technology, Roorkee, Uttarakhand-247667, India
[2]Civil and Environmental Engineering Department, Veermata Jijabai Technological Institute, Nathalal Parekh Marg, Matunga, Mumbai-400019, India
†Corresponding author: ssayyad@ce.iitr.ac.in, susayyad@ci.vjti.ac.in

Abbreviation: Nat. Env. & Poll. Technol.
Website: www.neptjournal.com

Received: 11-01-2024
Revised: 26-02-2024
Accepted: 16-03-2024

Key Words:

Aquaporin FO membrane
Draw solution concentration
Forward osmosis
Treated tannery effluent

Citation for the Paper:

Sayyad, S. U., 2025. Forward osmosis process for concentration of treated tannery effluent. *Nature Environment and Pollution Technology*, 24(1), B4144. https://doi.org/10.46488/NEPT.2025.v24i01.B4144.

Note: From year 2025, the journal uses Article ID instead of page numbers in citation of the published articles.

ABSTRACT

Forward Osmosis is a suitable pretreatment process for reverse osmosis for secondary-treated sewage reuse and secondary-treated industrial effluents. In this study, the FO process is investigated for concentrating synthetic secondary treated tannery effluents using 24 $g.L^{-1}$ and 38 $g.L^{-1}$ of NaCl solution as draw solution. Results showed that 38 $g.L^{-1}$ NaCl solution when used, provided higher flux and lower flux decline ratio as compared to 24 $g.L^{-1}$ NaCl solution. The solute rejection by FO membrane was more in FO experiments using 38 $g.L^{-1}$ NaCl solution as DS as compared to 24 $g.L^{-1}$ NaCl solution. Contact angle, Fourier transform infrared spectroscopy, and scanning electronic microscopy tests on pristine and chemically cleaned membranes indicated the change in membrane structure and the presence of foulants on the membrane surface, indicating insufficient chemical cleaning. Findings signify implications on the concentration of DS and the cleaning method adopted for concentrating treated tannery effluent efficaciously using the FO process.

INTRODUCTION

Leather making involves preparing hides/skins for tanning through pre-tanning operation, preservation of skin proteins permanently by tanning, and improving aesthetic properties during post-tanning stages. About 30-40 m^3 of wastewater is generated per ton of raw material processed. A variety of chemicals used for leather processing include sodium and ammonium salts, lime, fat liquors, antibiotics, tannins, dyes, etc. (Kaul et al. 2013). A portion of process chemicals ends up in the wastewater, generating a considerable amount of pollution load. The effluent treatment practice utilizes a conventional treatment system consisting of physico-chemical processes followed by biological methods. The conventional treatment system can remove pollutants such as Biochemical Oxygen Demand (BOD), Chemical Oxygen Demand (COD), and suspended solids. Often, resource recovery and water reuse are practiced in the industry to reduce the strength and quantity of wastewater produced. Biological treatment methods are practiced in the industry to remove total dissolved organics from wastewater. Even after treatment, the treated tannery wastewaters contain some amount of organic, nitrogenous matter and a high amount of total dissolved solids (TDS) (Pophali & Dhodapkar 2011, Ramteke et al. 2010).

The constituents contributing to TDS in tannery effluents are calcium, ammonium, magnesium, sodium, chlorides, nitrates, and sulfates. Such a treated effluent containing high TDS is not suitable for process and non-process reuse applications in the industry (Zhao et al. 2022). The effluent must be discharged to surface water, where strict limits are laid for chlorides and TDS parameters. Further, disposal of treated tannery effluent, high in chlorides and TDS, is reported to affect the fertility of the soil and contaminate groundwater, making the soil unsuitable

for agriculture and the water unfit for utilization purposes (Bhardwaj et al. 2023). Currently, Reverse Osmosis (RO) has been employed in tanning industries and common effluent treatment plants treating high TDS wastewater coming from the tannery industries (Ranganathan & Kabadgi 2011).

Suthanthararajan et al. (2004) investigated a pilot-scale case study of secondary treated tannery wastewater containing residual organic impurities and high concentrations of TDS, which are not removed by conventional treatment methods. A pilot plant membrane system designed for a capacity of 1 $m^3.h^{-1}$, consisting of nano and reverse osmosis (RO) membrane units, supported by pre-treatment operations of pressure sand filter, photochemical oxidizer, activated carbon filter, water softener, acid control, anti-oxidant, anti-scaling and cartridge filter, was analyzed to further treat and reuse the tannery wastewater. The maximum TDS removal efficiency of the polyamide RO membrane was above 98%. The permeate recovery of about 78% was achieved. The water recovered from the membrane system had a very low TDS concentration and was reused for the wet finishing process in the tanneries. The rejected concentrate obtained from the operation was sent to solar evaporation pans. Comparing the pre-treatment units, it was reported that most of the removal was achieved in the nanofiltration unit. The pre-treatment before the nano filter had little effect on the removal of organic and inorganic matter. The softener present in the system required periodical regeneration. The oxidizer and activated carbon filter were able to remove only 5 to 20% COD present in the influent. The sand media and cartridge filter were able to remove the suspended solids completely.

To improve the feed water quality of the RO system, the secondary treated tannery wastewater is passed through either conventional RO pre-treatment steps or Microfiltration (MF)/ Ultrafiltration (UF)/Nanofiltration (NF) membrane systems. Conventional pre-treatment processes to reverse osmosis treatment system consist of pH adjustment followed by a coagulation/flocculation process, disinfection, multimedia filtration, activated carbon filtration, and cartridge filtration (Jang et al. 2017, Pramanik et al. 2014, Sweity et al. 2013). In addition, membrane pre-treatment technologies like MF, UF, and NF are also practiced for Reverse Osmosis (Kim et al. 2002). All these methods increase the cost of the treatment and chemical usage.

In this context, Forward Osmosis (FO) may provide an effective alternative to pre-treatment to RO for treating the secondary tannery effluents. It is learned from the literature (Al-Zuhairi et al. 2015, Korenak et al. 2019, Thiruvenkatachari et al. 2016, Zaviska et al. 2015) that forward osmosis, when used as pre-treatment to RO, has the highest potential to reduce RO membrane fouling and scaling. This increases the life of the membranes, requires less chemical cleaning of membranes, and causes less damage to membranes during cleaning in the RO process. TDS removal from Tannery effluents is currently being accomplished in industries by RO process but comes under a high cost because of scaling, fouling, and damage of RO membranes, as discussed. Limited research is available for treating/concentrating tannery effluents with an FO system (Pal et al. 2017). Moreover, the researchers have often used cross-flow FO module configuration, which is quite an energy-intensive option, and no research is available on other FO module configurations used for treating secondary treated tannery effluent. In this study, we have evaluated the performance of the compartment configuration FO system in concentrating synthetic secondary treated tannery effluent. The objective of this research is as follows: 1. To investigate the performance of the FO process in terms of water flux, flux decline ratio, concentration factor, and contaminant rejection using synthetic secondary treated tannery effluent as feed solution. 2. Investigation of the effect of concentration of sodium chloride as a DS on contaminant rejection. 3. To investigate the FO membrane characteristics using different analytical techniques such as water contact angle (WCA), FTIR, SEM, and SEM-EDX.

MATERIALS AND METHODS

FO Membranes and Membrane Orientation

Aquaporin-embedded FO flat sheet membranes from Aquaporin Asia, Singapore, were purchased. The membranes were soaked in fresh deionized water and kept at 4ºC. Once a week, deionized water (DI) was replaced with fresh water. The membranes were washed in deionized water for at least 1 hour at room temperature before use. All studies were carried out with the active layer of the membrane towards the feed solution (FS).

Feed Solutions and Draw Solutions

The feed solution is either deionized water (DIW) or secondary treated tannery effluent. Synthetic secondary treated tannery effluent (SSTTE) solution simulating secondary treated real tannery effluents were prepared using Tannic acid (185 $mg.L^{-1}$), Peptone (100 $mg.L^{-1}$ $mg.L^{-1}$), NH_4Cl (1600 $mg.L^{-1}$), $CaSO_4$ (510 $mg.L^{-1}$), $MgSO_4$ $7H_2O$ (410 $mg.L^{-1}$), NaCl (6500 $mg.L^{-1}$), KCl (55 $mg.L^{-1}$), KNO_3 (40 $mg.L^{-1}$), Na_2SO_4 (5100 $mg.L^{-1}$) and $K_2Cr_2O_7$ (11.5 $mg.L^{-1}$) (Panizza & Cerisola 2004, Sundarapandiyan et al. 2010, Costa et al. 2010). To avoid bacterial growth in the SSTTE during the experimental duration, the SSTTE was autoclaved and cooled, and a dose of 6 $mg.L^{-1}$ ampicillin solution was added. The pH of the solution was adjusted

Table 1: Characteristics of synthetic secondary treated tannery effluent.

Parameter	Unit	SSTTE
pH	unitless	7.2-7.39
TDS	$mg.L^{-1}$	14147-14479.1
COD	$mg.L^{-1}$	326-336.10
Chlorides	$mg.L^{-1}$	4884.12-5072.39
Sulfates	$mg.L^{-1}$	3861.78-4191.75
Nitrates	$mg.L^{-1}$	21-22
Phosphates	$mg.L^{-1}$	6
Sodium	$mg.L^{-1}$	4420.85-4599.04
Potassium	$mg.L^{-1}$	51.34-57.73
Calcium	$mg.L^{-1}$	149.61-155.1
Magnesium	$mg.L^{-1}$	41.24-43.99
Ammonium	$mg.L^{-1}$	515.71-526.73
Total Chromium	$mg.L^{-1}$	3.7-4.07

using a 12 N NaOH solution. The characteristics of synthetic secondary treated tannery effluent are presented in Table 1.

The draw solution consisted of sodium chloride solutions of concentrations 24 $g.L^{-1}$ and 38 $g.L^{-1}$, respectively. The initial volume of the draw solution was 1000 mL for all experiments. The chemical reagents were purchased from S. D. Fine Chemical Ltd. and were of analytical grade. Ampicillin was purchased from HiMedia, Mumbai. A Millipore water purification system (Merck Millipore, 18.2 MΩ·cm at 25 ºC) provided deionized water (DIW), which was used for preparing the draw and feed solutions, rinsing the FO module at the end of the experiment and diluting samples for analysis.

Bench Scale Forward Osmosis Setup

Fig. 1a shows a schematic sketch of the bench size experimental setup used in this study, and Fig. 1b shows a photograph view of the experimental setup. The experiment was conducted in an air-conditioned room at 23 ± 1°C. This continuous flow apparatus is used to test the performance of the FO process under continuous feed solution supply and constant concentration draw solution conditions. The feed solution reservoir (1) supplies feed solution to the feed solution tank. To determine water flux owing to the FO process, the weight of the feed solution reservoir is monitored at time intervals. Weight was measured manually on a weight

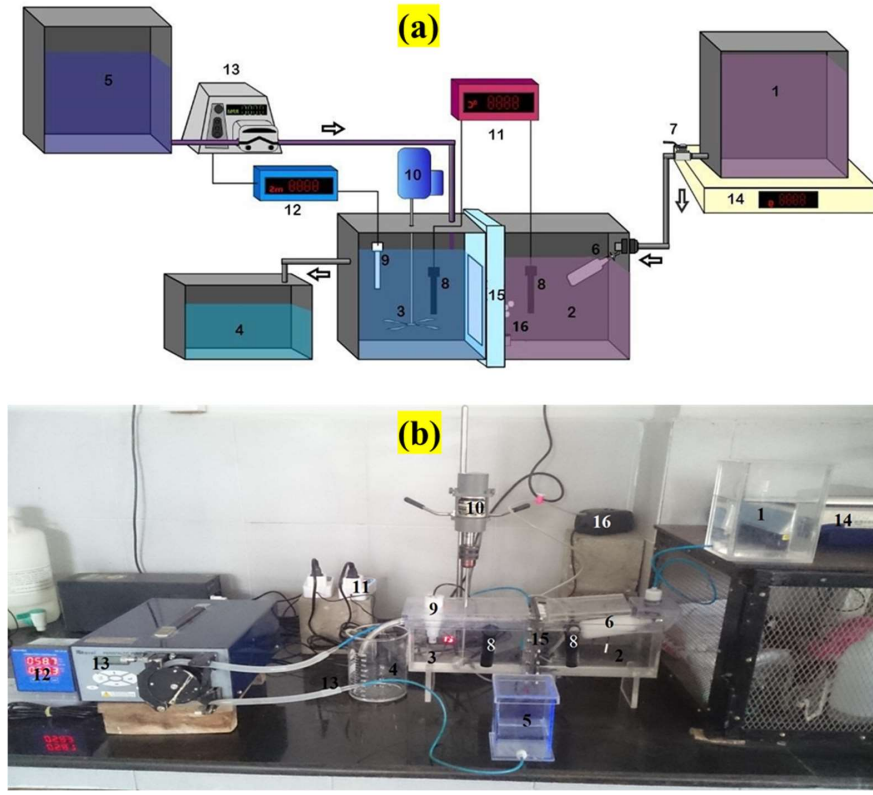

Fig. 1: Forward osmosis setup. a) Schematic diagram of the experimental setup, b) Photograph of the experimental setup. 1: Feed Solution Reservoir, 2: Feed Solution Tank, 3: Draw Solution Tank, 4: Separated Draw Solution Tank, 5: Concentrated Draw Solution Reservoir, 6: Float Valve 7: Flow Control Valve, 8: Heating Rods, 9: Conductivity Probe, 10: Stirrer, 11: Temperature Controller Unit, 12: Conductivity Controller Unit, 13: Peristaltic Pump, 14: Weigh Balance, 15: FO membrane Unit. 16: Aerator.

balance (14) (Citizen CTG, India). The aquaporin forward osmosis membrane vertically separates two acrylic tanks or compartments in this setup. The FO membrane is sealed to prevent leakage using a 3mm thick EPDM rubber sheet and 20 no's of 6 mm diameter stainless steel nuts and bolts. Out of the two compartments, the proper compartment (2) is of feed solution (which is deionized water/ wastewater), and the left compartment (3) is of draw solution, which is sodium chloride solution. The feed solution tank dimensions are 18.2cm length x 5.5cm width x 11cm height. The feed solution volume in the feed solution tank is maintained at 1 liter by providing a float valve (6) (MA052, Kerick, India) at the inlet of the feed solution tank. The effective membrane area is (8.5cm height x 4.0cm width) 34 cm^2. The feed solution faces the membrane's active layer. The volume of the feed solution is reduced while the volume of the draw solution is increased as pure water fluxes through the forward osmosis membrane. The float valve controls the rate at which feed solution is pumped into the feed solution tank from the feed solution reservoir.

The draw solution tank dimensions are 18.2cm × 5.5cm × 11cm. The draw solution volume used in the experiments is 1 L. The draw solution volume increases and dilutes due to pure water flux from the feed solution tank through the FO membrane. To collect and separate the increased draw solution volume, a 0.5mm diameter outlet port is provided to the draw solution tank at the height of 10 cm. The increased volume of the draw solution passes through the outlet port of the draw solution tank and gets collected in the separated draw solution tank (4). Thus, the draw solution volume in the draw solution tank is maintained constant. To maintain a constant concentration in the draw solution tank, a more concentrated draw solution (91.2 $g.L^{-1}$ sodium chloride solution) is supplied to the draw solution tank from the concentrated draw solution reservoir (5) by a peristaltic pump (13) (Ravel, India) which is connected to a conductivity controller (12) (MSCD09, MicroSet, India). The increase in conductivity of the water in the feed solution tank due to reverse solute flux is measured by a conductivity meter (Inolab Cond720, WTW Germany). A temperature control unit controls the temperature of the two compartments separated by a membrane. The temperature control unit consists of 2 nos of heating rods (8) (MINI-THERM, Cobalt International, SC) and 2 nos of temperature controllers (11) (XK-W2001, Robocraze, India). Mixing is done in the draw solution tank with the help of an axial impeller connected to a laboratory stirrer (10) (RQG-121-D, Remi Elektrotechnik Ltd, India). Feed solution mixing was carried out by diffusing air with the help of an aerator (16) (Eheim, Germany). The forward osmosis setup is unique in one way: this setup does not utilize pumps for the circulation of feed solution and draw solution.

Forward Osmosis Experimental Procedure

For the feed solution as SSTTE, we used 24 and 38 $g.L^{-1}$ of NaCl solution as the draw solution. All the experiments were conducted for 7 h. In all the experiments, aeration was done in the FS tank at a rate of 0.3 $mL.min^{-1}$, and mixing was done in the draw solution tank at a constant mixing rate of 75 RPM. For each experiment, a single membrane coupon is used. At the end of the experiment, the manufacturer-recommended procedure chemically cleaned the membrane coupon.

Calculation of Pure Water Flux, Flux Decline Ratio, Reverse Solute Flux, Concentration Factor, and Solute Rejection

The pure water flux J_w (LMH) was calculated using the equation (1) as given by (Dutta et al. 2022),

$$J_w = \Delta W/(\rho \times S_m \times \Delta t) \quad \ldots(1)$$

Where ΔW is the weight (g) change of the feed solution over a specific time Δt (hours.), ρ is feed solution density (assumed 1.0 $g.cm^{-3}$), and S_m is the effective membrane surface area (m^2). Further, the flux decline ratio FDR (%) was calculated using equation (2) as given by (Mondal & De 2015).

$$FDR = 100 - [(J_{w,f}/J_{w,i}) \times 100] \quad \ldots(2)$$

Where $J_{w,f}$ is the flux recorded at the end of the experiment, and $J_{w,i}$ is the initial recorded flux.

The concentration factor CF (%) was calculated as described by equation (3) as given by (Ortega-Bravo et al. 2016)

$$CF = 100\ (C_{f,Final}/C_{f,Initial}) \quad \ldots(3)$$

Where $C_{f,Final}$ is the final feed solution concentration ($mg.L^{-1}$) at the end of the experiment, and $C_{f,Initial}$ is the initial feed solution concentration ($mg.L^{-1}$).

Different ions in the feed solutions have been studied to determine their solute rejection factors. At the experiment's beginning and conclusion, the concentrations of ions in the draw and feed solutions were measured. Then, equation (4), as given by (Vital et al. 2018), was used to determine solute rejection SR (%).

$$SR = [(C_{f,Initial} - C_p)/C_{f,Initial}] \times 100 \quad \ldots(4)$$

Where $C_{f,Initial}$ represents the initial concentration ($mg.L^{-1}$) of the ion on the feed side, and C_p is the concentration ($mg.L^{-1}$) of the ion on the permeate (draw side). Concentration (mg/L) on the permeate C_p is evaluated using equation (5) as given by (Vital et al. 2018)

$$C_p = (C_d \times V_d)/V_p \quad \ldots(5)$$

Where C_d is the concentration ($mg.L^{-1}$) on the draw side, V_d is the volume (L) of the draw solution by the end of the experiment, and V_p is the volume (L) of water that permeates from the feed to the draw side.

Sampling and Analytical Methods

Feed solution (synthetic secondary treated tannery effluent) in the feed solution tank was collected before the start and after the completion of the experiment. Draw solution samples were collected at the end of the experiment for analysis. The feed solution samples were analyzed for COD, EC, Total Chromium, cations (Sodium, Ammonium, Potassium, Magnesium, and Calcium), and anions (Chlorides, Nitrates, Orthophosphates, and Sulphates). The draw solution samples were analyzed for Total Chromium, cations, and anions.

In brief, COD was determined (Aqualytic AL38SC) by a closed reflux colorimetric method according to Standard Methods for the Examination of Water and Wastewater. COD levels were determined by measuring the absorbance of the digested solution at 600nm on a Hach DR-6000 UV-visible spectrophotometer. Ion Chromatography determined cations (Sodium, Ammonium, Potassium, Magnesium, and Calcium) and anions (Chlorides and Sulphates) with chemical suppression of eluent conductivity (Metrohm, 850 Professional IC). Nitrate was measured as Nitrate-N by ultraviolet spectrophotometric screening method (APHA 4500). Phosphate was measured by the stannous chloride method (APHA 4500-P D). Further cation (Magnesium, Potassium, Total Chromium) concentrations in the DS were also analyzed using an inductively coupled plasma-optical emission spectrometer (ICP-OES, Agilent 700).

Membrane Characterization

At the NCNNUM laboratory in Mumbai, the Rame-hart contact angle instrument is used to measure the contact angle to quantify the hydrophobicity/hydrophilicity of virgin and chemically treated membranes. The membranes were air-dried at room temperature before contact angle measurements using the Sessile Drop Technique or Static Contact Angle measurements. The contact angles reported are the average of 7-9 measurements made with pure water droplets. The changes in the chemical structure of the samples were investigated using attenuated total reflection-Fourier transform infrared spectroscopy (ATR-FTIR, make: PerkinElmer (USA), L1600400 Spectrum TWO DTGS) at a resolution of 4 cm^{-1}. On samples of clean and chemically cleaned membranes, ATR/FTIR analysis was carried out. There are 20 scans with a wavelength range of 600-4000 cm^{-1} were used to examine the spectra. To achieve a similar close contact between the ATR crystal and sample surface, all samples were pressed down with the same amount of pressure. The FO membrane was examined using scanning electron microscopy (SEM) ((Carl Zeiss Model: Zeiss Gemini SEM) and energy-dispersive X-ray spectroscopy (EDX) (EDAX APEX). Surface and cross-sectional imaging were performed on clean membranes, and surface imaging was on chemically cleaned membranes. Coupons were dipped in liquid nitrogen and cut using a razor to show the membrane cross-section. Samples were sputtered with gold before SEM imaging to prevent charging of the non-conductive membrane surface.

RESULTS AND DISCUSSION

Water Flux and Flux Decline Ratio

Fig. 2 shows the change of flux as a function of time under FO mode using SSTTE as FS and 24 $g.L^{-1}$ and 38 $g.L^{-1}$ of NaCl solution as DS. When the DS concentration was 24 $g.L^{-1}$ and 38 $g.L^{-1}$ of NaCl solution, the initial flux values for SSTTE were 4.41 LMH and 7.44 LMH, respectively. Experiments with lower DS concentration have lower initial flux, while experiments with higher DS concentration have higher initial flux (Camilleri-Rumbau et al. 2019). However, with respect to time, the flux declines in experiments for DS concentrations of 24 $g.L^{-1}$ and 38 $g.L^{-1}$ NaCl solution. The first rapid decline in flux is mainly because of fouling, while further, the flux declines due to the combined effects of fouling, the concentration of FS, and the back diffusion of DS (Han et al. 2016). All this process is slower in lower DS concentration (24 $g.L^{-1}$ of NaCl solution) experiments, while this is faster in higher DS concentration (38 $g.L^{-1}$ of NaCl solution) experiments (Nguyen & Yoshikawa 2019). The flux values at the end of the experiment for SSTTE were 2.41 LMH and 5.44 LMH when the DS concentration was 24 $g.L^{-1}$ and 38 $g.L^{-1}$ of NaCl solution, respectively.

The flux decline ratio was calculated using equation (2). The initial flux decline ratio is low (5.21%) in lower DS concentration (24 $g.L^{-1}$ of NaCl solution) experiments, whereas the initial flux decline ratio is more (9.14%) in higher DS concentration (38 $g.L^{-1}$ of NaCl solution) experiments for FS as SSTTE (Morrow & Childress 2019). Fig. 3 shows that the flux decline ratio at the end of the experiment (7 hours) when using 24 $g.L^{-1}$ and 38 $g.L^{-1}$ NaCl solution as against SSTTE was 45.35% and 26.88%, respectively, whereas the average flux was 3.54 LMH and 6.175 LMH respectively. The flux decline ratio at the end of the experiment is more in the low DS concentration (24 $g.L^{-1}$ of NaCl solution) experiment, whereas it is less in the high DS concentration (38 $g.L^{-1}$ of NaCl solution) experiment. In hydraulic pressure-driven membrane processes, higher values of flux decline ratio indicate that the membrane has fouled more (Conidi et al. 2019). However, in FO processes where hydraulic pressure is not used, this may not be true. In the FO process, though, flux decline is slower in the low DS experiment than in the high DS experiment, but operating the

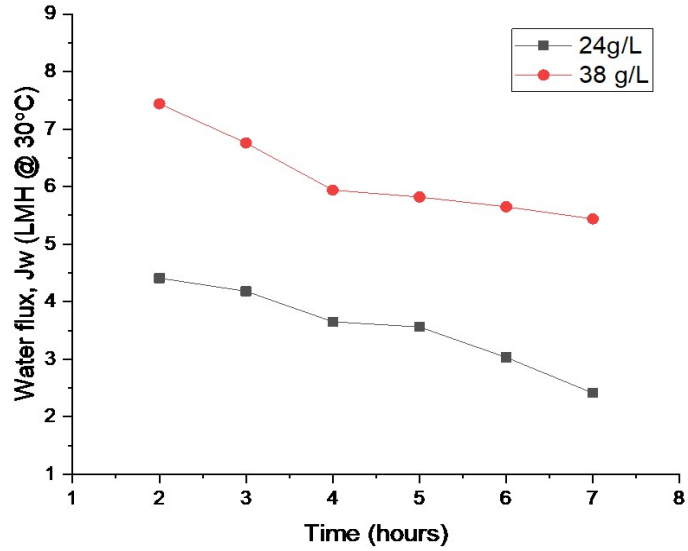

Fig. 2: Effect of draw solution concentration on pure water flux. FS is synthetic secondary treated tannery wastewater. DS concentration is 24 and 38 g.L^{-1} NaCl solution, respectively. DS concentration is kept constant throughout the experimental duration. All experiments are conducted at a constant temperature of 30°C. The membrane's active layer is facing towards the feed solution.

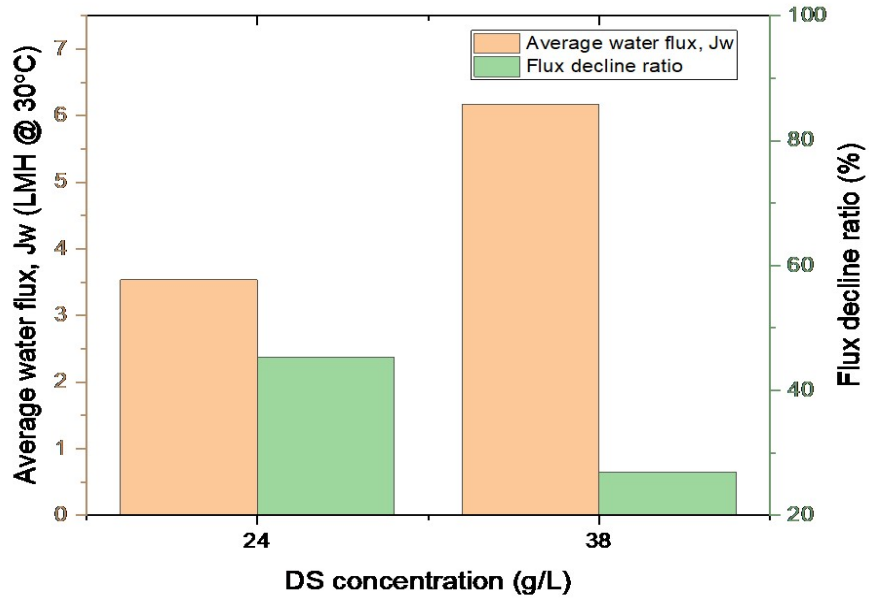

Fig. 3: Effect of draw solution concentration on average pure water flux and flux decline ratio. FS is synthetic secondary treated tannery wastewater. DS concentration is 24 and 38 g.L^{-1} NaCl solution, respectively. DS concentration is kept constant throughout the experimental duration. All experiments are conducted at a constant temperature of 30°C. The membrane's active layer is facing towards the feed solution.

FO process at low DS concentration has a greater impact on flux. A slight decrease in osmotic pressure gradient decreases the flux largely, especially at low DS concentrations, as compared to high DS concentrations, as the flux vs osmotic pressure curve is non-linear (Lay et al. 2012). The flux declines largely in low DS experiment as compared to high DS experiment because of fouling, then decrease in osmotic pressure gradient due to concentration of FS, back diffusion of DS (RSF), and cake-enhanced osmotic pressure (CEOP) (Gao et al. 2018).

The low flux decline ratio (26.88%) in the experiment with SSTTE and 38 g.L^{-1} NaCl solution is mainly attributed to the high DS concentration in the DS tank (38 g.L^{-1} NaCl solution). At higher DS concentrations, flux is not impacted

by slight changes in the osmotic pressure gradient (Lay et al. 2012). Further the flux is also enhanced due to the novel FO module configuration used in this study. Mixing in the DS tank of the FO module configuration provides a uniform concentration of DS in the DS tank, while the configurations using pumps to circulate draw solution like the cross-flow configurations, plate and frame configuration, and hybrid dead-end cross-flow configuration, the concentration of draw solution at inlet and outlet are varying (Sagiv et al. 2014). Therefore, in these configurations, the entire effective area of the membrane will not be subjected to a uniform transmembrane pressure, resulting in a decreasing flux along the length of the membrane (Gruber et al. 2012).

Concentration Factor

Concentration factors (%) were calculated using equation (2.3). Concentration factors (CF) represent the percentage of the value of a specific parameter that increases or decreases due to the concentration process. When a parameter decreases, CF is presented as negative to emphasize that the parameter experienced a reduction. The greater the concentration gradient between FS and DS, the greater the FS concentration (Ortega-Bravo et al. 2016). Fig. 4 shows the concentration factors for Calcium, Magnesium, Potassium, Sodium, Ammonium, Electrical Conductivity (EC), Chlorides, Sulphates, Nitrates, Phosphates, COD and Total Chromium (Total Cr). Calcium concentration increased

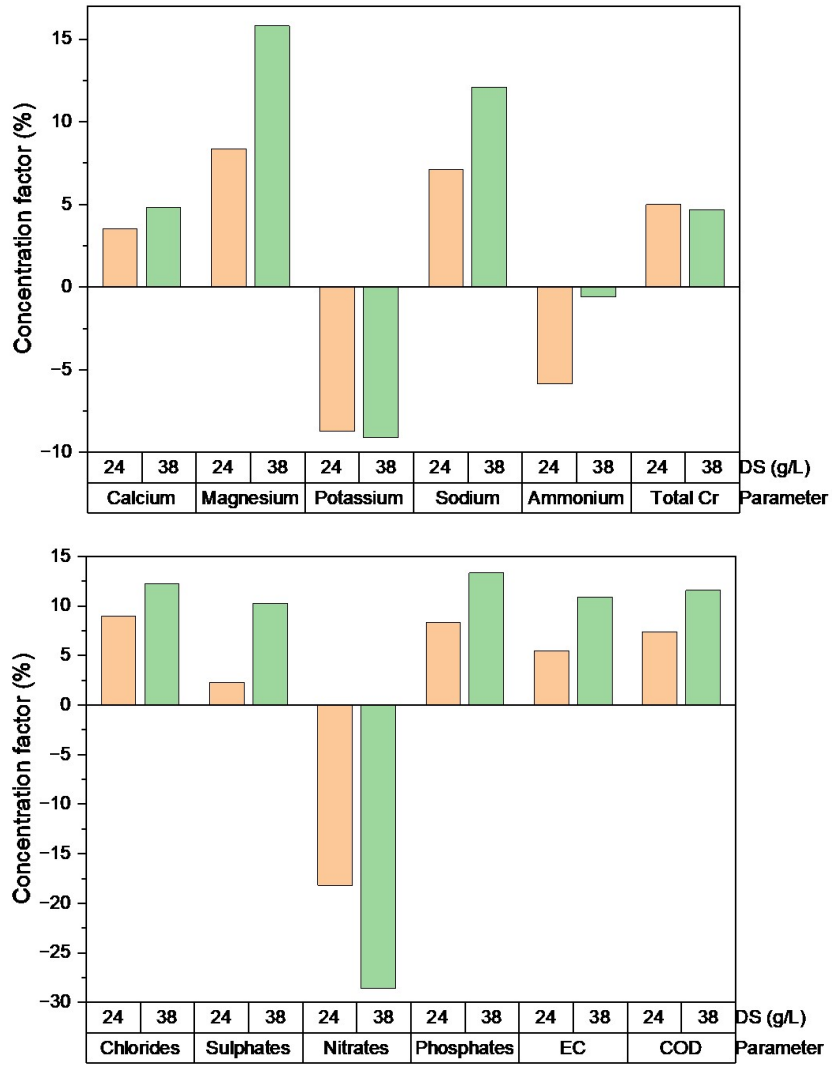

Fig. 4: Percentage change in concentration of FS parameters due to the Forward Osmosis process. FS is synthetic secondary treated tannery wastewater. DS concentration is 24 and 38 g.L^{-1} NaCl solution, respectively. DS concentration is kept constant throughout the experimental duration. All experiments are conducted at a constant temperature of 30 ºC. The membrane's active layer is facing toward the feed solution.

in SSTTE by 3.53% and 4.83% in experiments when DS was 24g.L^{-1} and 38 g.L^{-1} NaCl solution, respectively. When a mass balance was conducted, the experimental final concentration value differed from the theoretical values. The possible reason might be that calcium might have formed bonds with the negatively charged membrane surface and with other ions and precipitated on the membrane surface (Duong & Chung 2014). Magnesium concentration increased in SSTTE by 8.34% and 15.81% in experiments when DS was 24 g.L^{-1} and 38 g.L^{-1} NaCl solution, respectively. When a mass balance was conducted, the experimental final concentration value matched near the theoretical values. This verified that magnesium precipitation had not occurred on the membrane in 24 g.L^{-1} and 38 g.L^{-1} DS experiments. Magnesium has a high affinity towards Chlorides and Sulphates and must have formed a bond with Chlorides and Sulphates (Gao et al. 2018). Concentration factors for Potassium showed negative values of 8.73% and 9.10% in experiments when DS was 24g.L^{-1} and 38 g.L^{-1} NaCl solution, respectively. The possible reason might be the low hydrated radius of Potassium and the low capacity of the membrane to retain Potassium in the FS compartment, or it could be the transport of Potassium to DS due to the Donnan equilibrium effect. The Donnan equilibrium effect says that if an ion is having high affinity towards another ion than the one with which it is currently attached, then the ion will break the bond and join the bond with the ion with which it has high affinity. Sodium concentration increased in SSTTE by 7.12% and 12.1% in experiments when DS was 24g.L^{-1} and 38 g.L^{-1} NaCl solution respectively. When a mass balance was conducted the experimental final concentration value matched near to the theoretical values. Since FS contained a high concentration of sodium and the selected DS was also a NaCl solution so sodium flux from DS to FS was negligible. Likewise, Potassium the concentration factors for Ammonium showed negative values of 5.87% and 0.60% in experiments when DS was 24g.L^{-1} and 38 g.L^{-1} NaCl solution respectively. The possible reason might be the high diffusion coefficient, the low hydrated radius of ammonium, and the low capacity of the membrane to retain ammonium in the FS compartment, or could be the transport of ammonium to DS due to the Donnan equilibrium effect (Ortega-Bravo et al. 2016).

The total Chromium concentration factor in SSTTE is 5% and 4.67% for experiments when DS was 24 g.L^{-1} and 38 g.L^{-1} NaCl solution, respectively. This is because, in the case of higher DS concentration, the Total Chromium must have either been precipitated on the membrane or Total Chromium must have been transported to DS (Pham et al. 2021). Chloride concentration increased in SSTTE by 8.97% and 12.25% in experiments when DS was 24 g.L^{-1} and 38 g.L^{-1} NaCl solution, respectively. When a mass balance was conducted, the experimental final concentration value matched near the theoretical values. Sulfate concentration increased in SSTTE by 2.27% and 10.23% in experiments when DS was 24 g.L^{-1} and 38 g.L^{-1} NaCl solution, respectively. It is seen the concentration of Sulphates in the final FS is lower than the values obtained from the mass balance in experiments when DS was 24 g.L^{-1} and 38 g.L^{-1} NaCl solution. The possible reason might be the bonds formed with Calcium and Magnesium and precipitation on the membrane surface (Hancock et al. 2011, She et al. 2012). Concentration factors for Nitrates showed negative values of 18.18% and 28.57% in experiments when DS was 24 g.L^{-1} and 38 g.L^{-1} NaCl solution, respectively. The possible reason might be the high diffusion coefficient, the low hydrated radius of Nitrates, and the low capacity of the membrane to retain Nitrates in the FS compartment, or it could be the transport of nitrates to DS due to the Donnan equilibrium effect (Damirchi & Koyuncu 2021). Phosphate concentration increased in SSTTE by 8.33% and 13.33% in experiments when DS was 24 g.L^{-1} and 38 g.L^{-1} NaCl solution, respectively. When a mass balance was conducted, the experimental final concentration value matched near the theoretical values. The possible reason might be the large hydrated radius of negatively charged phosphate ions accumulated in the FS (Luo et al. 2018). For increasing DS concentration, the conductivity increase was high. When DS was 24 and 38 g.L^{-1} of NaCl solution, the SSTTE conductivity increased by 5.45% and 10.86%, respectively. Similarly, the COD increase in SSTTE was 7.36% and 11.57% when DS was 24 g.L^{-1} and 38 g.L^{-1} NaCl solution, respectively. This increase in concentration during the FO process is due to the addition of FS from the FS reservoir during the FO process (Hickenbottom et al. 2013).

Solute Rejection

The rejection of the ions under the FO system could be attributed to several reasons. (1) Because no pressure is applied in the FO process, the effect of convective flow on the ion transport is insignificant. (2) The Donnan equilibrium effect may also contribute to the high rejections under the FO process.

Fig. 5 showed the rejection of Total Chromium, Magnesium, Potassium, and Ammonium ions by the FO membrane when FS was SSTTE and DS was 24 g.L^{-1} and 38 g.L^{-1} of NaCl solution, respectively. ICPOES determined all the ions except ammonium. Chromium ions were rejected at 86.23% and 96.22% when DS was 24 g.L^{-1} and 38 g.L^{-1} of NaCl solution, respectively. The hydrated radius of chromium ion is 0.461 nm and, therefore, is well rejected

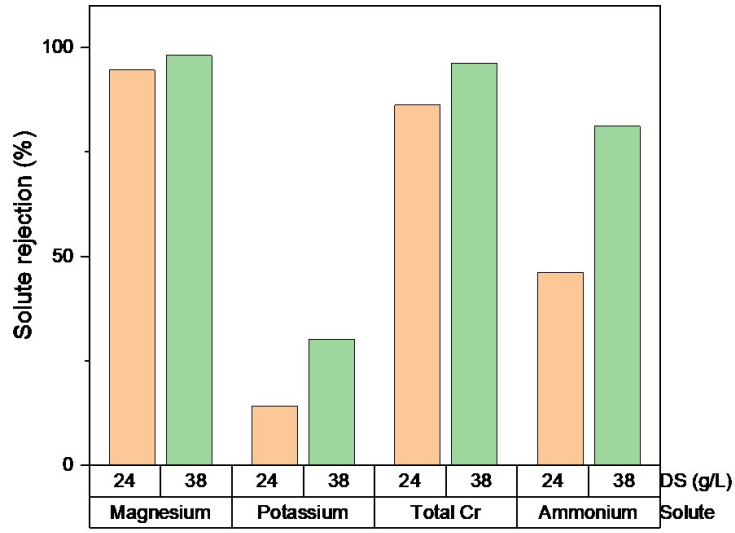

Fig. 5: Solute rejection by FO membrane. FS1 is synthetic secondary treated tannery wastewater with a concentration of 14 $g.L^{-1}$. DS concentration is 28 and 38 $g.L^{-1}$ NaCl solution, respectively. DS concentration is kept constant throughout the experimental duration. All experiments are conducted at a constant temperature of 30 ºC. The membrane's active layer is facing towards the feed solution.

by the FO membrane (Pham et al. 2021). The rejection for Magnesium ion was 94.56% and 98.13% when DS was 24 $g.L^{-1}$ and 38 $g.L^{-1}$ of NaCl solution, respectively. Magnesium rejection was more significant at high DS concentrations. Magnesium is well rejected due to size exclusion because it is a divalent cation with a larger hydrated radius (0.428 nm) than the pore size of the FO membrane (Coday et al. 2015, Gao et al. 2018). The rejection of Potassium is 14.17 and 30.25% when DS was 24 $g.L^{-1}$ and 38 $g.L^{-1}$ of NaCl solution, respectively. The rejection of potassium was higher for higher DS concentrations. Furthermore, potassium, a monovalent ion with a low hydrated radius (0.331nm) and more excellent water permeability is less rejected by FO membranes irrespective of the FS concentration (Hancock et al. 2011, Roy et al. 2016). Likewise, in Potassium, the rejection of Ammonium was lower and was 46.15% and 81.16% when DS was 24 $g.L^{-1}$ and 38 $g.L^{-1}$ of NaCl solution, respectively. However, it is notable that the rejection of Potassium and Ammonium was higher when a 38 $g.L^{-1}$ NaCl solution was used as DS as compared to a 24 $g.L^{-1}$ NaCl solution.

Membrane Characterization

The pristine and chemically cleaned membrane was analyzed for contact angle, ATR-FTIR, SEM, and SEM EDX to determine if the membrane surface underwent modification due to the chemical cleaning. The chemical cleaning was done only on the active layer side of the membrane. The chemical cleaning was done using an alkaline-acid cleaning method. The alkaline solution would remove the organic foulants on the membrane, and the acid solution would remove the inorganic constituents. Alkaline cleaning at 30ºC with 0.001 M NaOH solution (pH=11) for 30 min, followed by acid cleaning at 30 ºC with 0.01 M HNO_3 (pH = 2) for 30 min, was done to clean the membrane chemically.

Contact Angle

A surface is hydrophobic when its static water contact angle θ is >90° and is hydrophilic when θ is <90°. At 25°C, DI water was used as the probe liquid in a contact angle goniometer to assess the hydrophilicity of aquaporin membranes' active and support layers. The contact angle was recorded within 10 seconds of a small water droplet deposition on the flat membrane surface. The contact angle was measured from at least five random points to limit the influence of surface heterogeneity. The average value was then reported. The contact angle was measured for the new membrane and chemically cleaned membrane. The contact angle measurements for the active and support layers are given in Table 2.

Table 2: Contact angle values of pristine and chemically cleaned aquaporin forward osmosis membrane.

Membrane Layer	Contact angle		Reference
	Pristine FO membrane	Cleaned FO membrane	
Active layer	59.28±0.05º	52.66 ±0.05º	This study
Support layer	75.71º	58.91º	This study
Active layer	53º	---	(Omir et al. 2020)
Support layer	61º	---	

The contact angle values of the pristine membranes' active layer and support layer suggest that the active layer is more hydrophilic than the support layer. When the membrane was exposed to chemical cleaning, the contact angle of the active layer decreased from 59.28º to 52.66º. No chemical cleaning of the support layer was done. However, the contact angle of the support layer changed from 75.71º to 58.91º, making the support layer more hydrophilic. These results indicate that accumulating chemical cleaning agents on the membrane's surface increases membrane hydrophilicity. The increased hydrophilicity thus improves the flux performance of the membranes (Tasci et al. 2022).

Attenuated Total Reflectance-Fourier Transform Infrared Spectroscopy (ATR-FTIR)

ATR-FTIR spectra of a pristine and chemically cleaned aquaporin membrane's active layer were observed to identify any significant change in the chemical structure. Fig. 6a and Fig. 6b show the FTIR spectra of pristine and chemically cleaned membranes. Fig. 6a shows the FTIR spectrum of the pristine membrane. The active layer of the pristine membrane is fully polyamide. FTIR spectrum showed characteristic peaks at 1656.99 cm^{-1}, 1577.79 cm^{-1}, and 1485.65 cm^{-1}, which suggested the selective layer of the aquaporin membrane was fully aromatic polyamide. Peaks at wave numbers 2854.41 cm^{-1} and 2925.01 cm^{-1} of the FTIR spectrum demonstrated the presence of the lipid tails of aquaporin protein. These peaks confirmed the incorporation of aquaporin proteins into the membrane-selective layer. The peak at 1743.34 cm^{-1} suggested the occurrence of the phosphate I band from the lipid bilayer of the aquaporin vesicles. The lipid tails of aquaporin protein were confirmed from peaks at wave numbers 2854.41 cm^{-1} and 2925.01 cm^{-1}. Fig. 6b shows the FTIR spectrum of the chemically cleaned membrane. After chemical cleaning, a significant change was observed in the FTIR spectrum at 3293.16 cm^{-1}, 1652.51 cm^{-1}, and 1372.93 cm^{-1}. This demonstrates that there must still be some foulants on the membrane (Khraisheh et al. 2020), or the chemicals used for cleaning the membrane must have changed the structure of the membrane (Li et al. 2017).

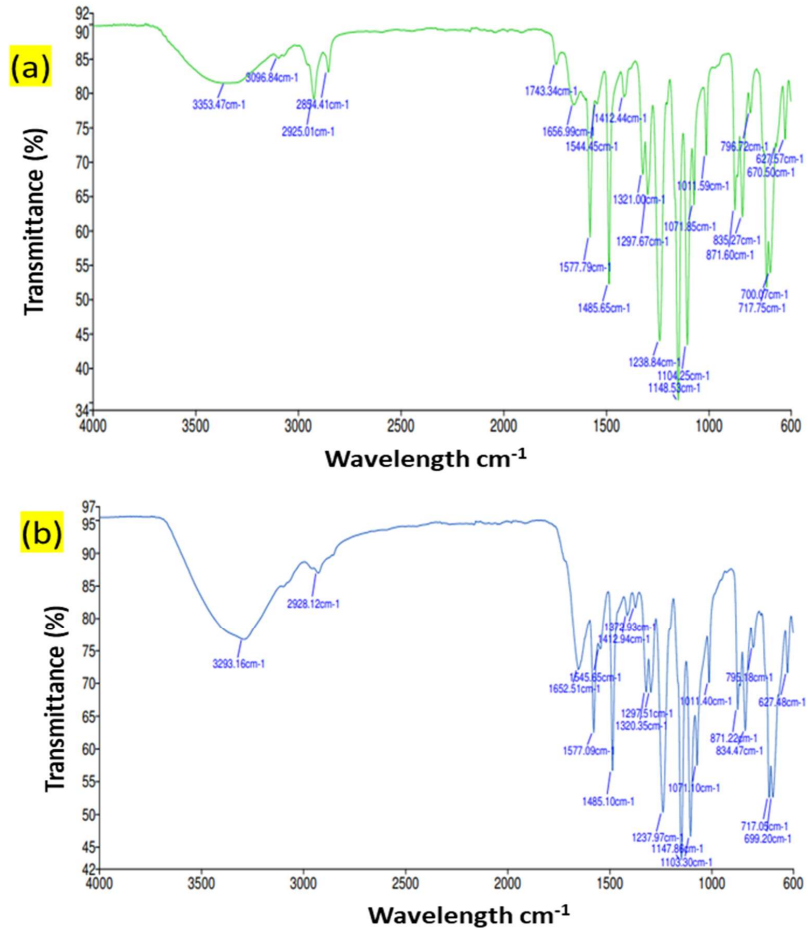

Fig. 6: FTIR spectrum of the a) pristine membrane and b) chemically cleaned membrane.

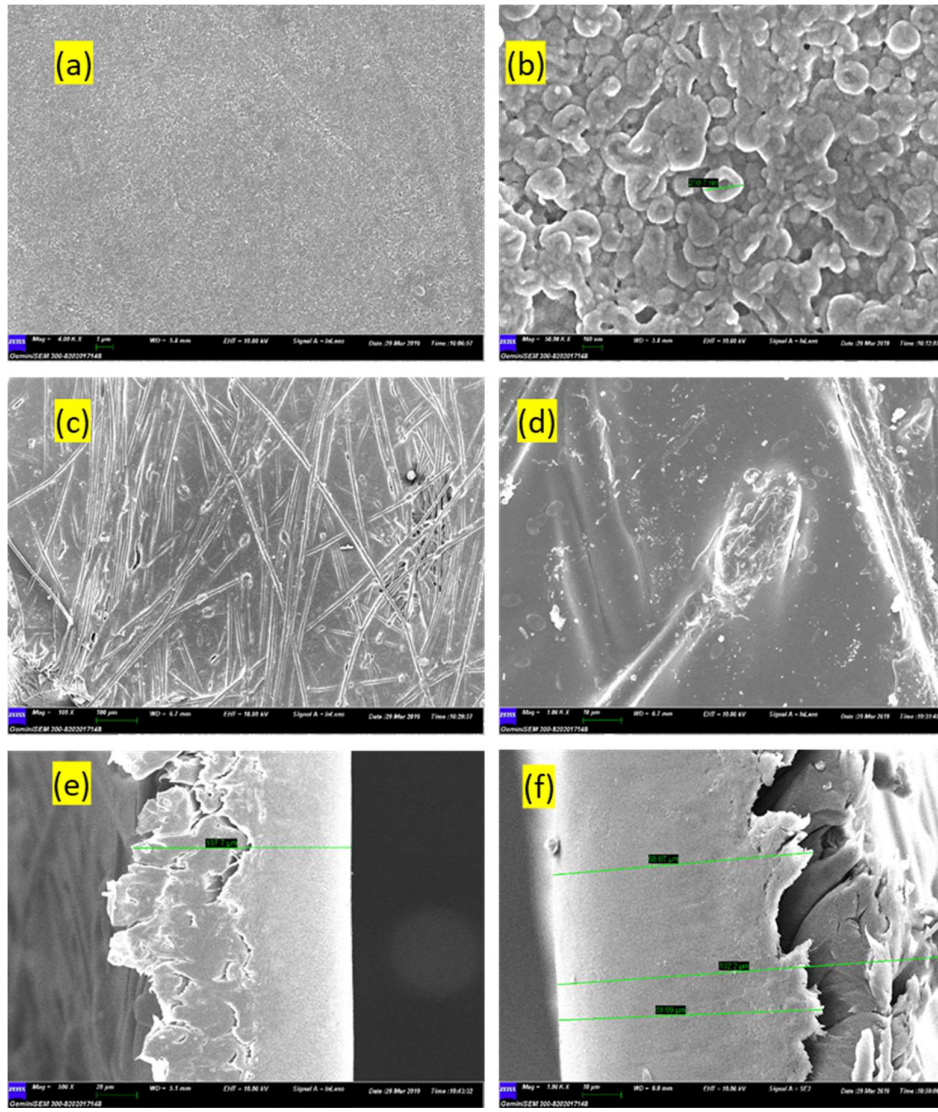

Fig. 7: SEM images of aquaporin-based forward osmosis pristine membrane at 10 kV a) active layer (AL) (magnification×4k) b) active layer (AL) with incorporated aquaporin vesicles(~210 nm) (magnification ×50k), c) support layer (SL) (magnification ×100), d) support layer (SL) (magnification×1k), e) cross-section (magnification×500), f) cross-section (magnification ×1k).

Scanning Electron Microscopy (SEM) and Energy Dispersive X-Ray Analysis (EDX)

Aquaporin vesicles with a round form were seen in the active membrane layer according to membrane cross-section morphology. Fig. 7 showed the existence of circular nodules with an estimated size of 100 nm at the membrane interface, comparable to the size of a proteoliposome containing aquaporin protein (Li et al. 2014). The aquaporin proteins were embedded in the active layer of AQP, which resulted in a porous structure for the active layer. All the membranes' cross-sections showed asymmetric structures, often resulting from the phase-inversion process.

Fig. 8 shows the SEM EDX analysis for the chemically cleaned membrane. To confirm that the foulant particles have been removed from the active layers of the aquaporin membrane, the active surfaces were characterized by SEM combined with EDX. The SEM images illustrated the adsorption of foulant particles on FO membranes after chemical cleaning. The EDX analysis confirms the presence of carbon (C), sulfur (S), and oxygen (O). However, this reveals the organic nature of the membranes to more extent. Traces of calcium (Ca) and magnesium (Mg) are seen throughout the examined membrane surfaces since the FS contained calcium and magnesium that must have been attached to the membrane surface and not removed after

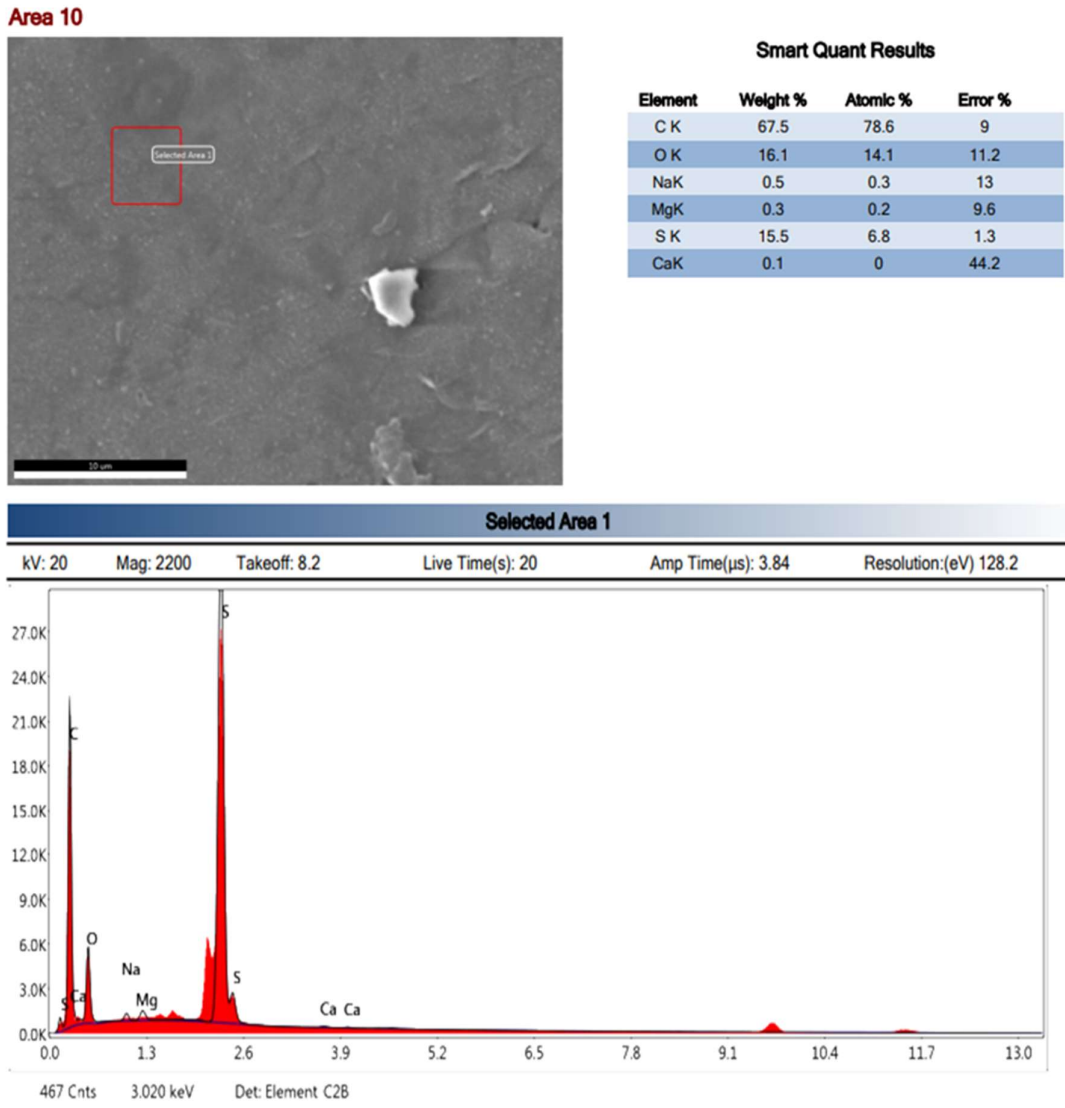

Fig. 8: SEM EDX spectra of the active layer of the chemically cleaned membrane.

chemical cleaning. The membrane's support layer possibly contained trapped sodium chloride, so a sodium peak was also found in the EDX analysis. This suggests the chemical cleaning method does not ensure 100% membrane cleaning.

CONCLUSIONS

A novel compartment configuration FO membrane system was built up for concentrating synthetic secondary treated tannery effluent. Membrane flux was affected by DS concentration. Experiments revealed higher fluxes and lower flux decline ratio for 38 $g.L^{-1}$ NaCl solution as DS when compared with 24 $g.L^{-1}$ NaCl solution, indicating its convenience for concentrating SSTTE. Concentration factors for ions like calcium, magnesium, sodium, chlorides, sulfates, phosphates, and total chromium were positive, whereas ions like ammonium, potassium, and nitrates had negative concentration factors. Results indicated FO membrane had an excellent rejecting effect. Ions like magnesium and total chromium were largely rejected, whereas ions like ammonium and potassium were less rejected. Solute rejection was affected by DS concentration. Experiments with 24 $g.L^{-1}$ NaCl solution as DS showed low rejection of ions as compared to experiments with 38 $g.L^{-1}$ NaCl solution as DS. FO membrane had low fouling potential, with a fouling layer consisting of humic acid, protein, and polysaccharide. Fouled FO membrane was cleaned by chemical cleaning but still showed foulant deposits recommending more study on membrane cleaning procedures.

NOMENCLATURE

Description	Notation	Unit
Concentration of Draw Solution	C_d	$g.L^{-1}$
Concentration of Feed Solution	C_f	$g.L^{-1}$
Deionized Water	DIW	
Draw Solution	DS	
Effective Membrane Area	S_m	m^2
Feed Solution	FS	
Flux decline ratio	FDR	%
Forward Osmosis	FO	
Internal Concentration Polarization	ICP	
Pure Water Flux	J_w	LMH
Reverse Osmosis	RO	
Reverse Solute Flux	J_s	GMH
Sodium Chloride Solution	NaCl	$g.L^{-1}$
Thin Film Composite	TFC	
Density of Water	ρ	$kg.L^{-1}$
Temperature	T	℃
Concentration of ions on the permeate side	C_p	$mg.L^{-1}$
Volume of permeate from feed to draw side	V_p	L
Volume of DS at the end of the experiment	V_d	L
Concentration polarization	CP	
Concentration factor	CF	
Chemical Oxygen Demand	COD	$mg.L^{-1}$
Biochemical Oxygen Demand	BOD	$mg.L^{-1}$
Total Dissolved Solids	TDS	$mg.L^{-1}$
Synthetic secondary treated tannery effluent	SSTTE	
Solute rejection	SR	%

ACKNOWLEDGMENTS

Sameer Sayyad wishes to acknowledge the support received from the Quality Improvement Programme Cell, IIT Roorkee, and All India Council of Technical Education, INDIA, for this research work. Sameer Sayyad wishes to acknowledge the support received from Dr Pramod Kumar (Late), Associate Professor, Civil Engineering Department, IIT Roorkee.

REFERENCES

Al-Zuhairi, A., Merdaw, A.A., Al-Aibi, S., Hamdan, M., Nicoll, P., Monjezi, A.A., Al-ASwad, S., Mahood, H.B., Aryafar, M. and Sharif, A.O., 2015. Forward osmosis desalination from laboratory to market. *Water Supply*, 15(4), pp.834-844. https://doi.org/10.2166/ws.2015.038

Bhardwaj, A., Kumar, S. and Singh, D., 2023. Tannery effluent treatment and its environmental impact: A review of current practices and emerging technologies. *Water Quality Research Journal*, 58(2), pp.128-152. https://doi.org/10.2166/wqrj.2023.002

Camilleri-Rumbau, M.S., Soler-Cabezas, J.L., Christensen, K.V., Norddahl, B., Mendoza-Roca, J.A. and Vincent-Vela, M.C., 2019. Application of aquaporin-based forward osmosis membranes for processing of digestate liquid fractions. *Chemical Engineering Journal*, 371, pp.583-592. https://doi.org/10.1016/j.cej.2019.02.029

Coday, B.D., Almaraz, N. and Cath, T.Y., 2015. Forward osmosis desalination of oil and gas wastewater: Impacts of membrane selection and operating conditions on process performance. *Journal of Membrane Science*, 488, pp.40-55. https://doi.org/10.1016/j.memsci.2015.03.059

Conidi, C., Fucà, L., Drioli, E. and Cassano, A., 2019. A membrane-based process for the recovery of glycyrrhizin and phenolic compounds from licorice wastewaters. *Molecules*, 24(12), pp.2279. https://doi.org/10.3390/molecules24122279

Costa, C.R., Montilla, F., Morallón, E. and Olivi, P., 2010. Electrochemical oxidation of synthetic tannery wastewater in chloride-free aqueous media. *Journal of Hazardous Materials,* 180(1–3), pp.429-435. https://doi.org/10.1016/j.jhazmat.2010.04.048

Damirchi, M. and Koyuncu, I., 2021. Nutrient recovery from concentrated municipal wastewater by forward osmosis membrane and MgCl2 based draw solution. *Desalination and Water Treatment*, 211, pp.448-455. https://doi.org/10.5004/dwt.2021.26788

Duong, P.H.H. and Chung, T.-S., 2014. Application of thin film composite membranes with forward osmosis technology for the separation of emulsified oil–water. *Journal of Membrane Science*, 452, pp.117-126. https://doi.org/10.1016/j.memsci.2013.10.030

Dutta, S., Dave, P. and Nath, K., 2022. Choline chloride-glycerol (1:2 mol) as draw solution in forward osmosis for dewatering purposes. *Membrane and Water Treatment*, 13(2), pp.63-72. https://doi.org/10.12989/MWT.2022.13.2.063

Gao, Y., Fang, Z., Liang, P. and Huang, X., 2018. The direct concentration of municipal sewage by forward osmosis and membrane fouling behavior. *Bioresource Technology*, 247, pp.730-735. https://doi.org/10.1016/j.biortech.2017.09.145

Gruber, M.F., Johnson, C.J., Tang, C., Jensen, M.H., Yde, L. and Hélix-Nielsen, C., 2012. Validation and analysis of forward osmosis CFD model in complex 3D geometries. *Membranes*, 2(4), pp.764-782. https://doi.org/10.3390/membranes2040764

Han, G., Liang, C.-Z., Chung, T.-S., Weber, M., Staudt, C. and Maletzko, C., 2016. Combination of forward osmosis (FO) process with coagulation/flocculation (CF) for potential treatment of textile wastewater. *Water Research*, 91, pp.361-370. https://doi.org/10.1016/j.watres.2016.01.031

Hancock, N.T., Phillip, W.A., Elimelech, M. and Cath, T.Y., 2011. Bidirectional permeation of electrolytes in osmotically driven membrane processes. *Environmental Science & Technology*, 45(24), pp.10642-10651. https://doi.org/10.1021/es202608y

Hickenbottom, K.L., Hancock, N.T., Hutchings, N.R., Appleton, E.W., Beaudry, E.G., Xu, P. and Cath, T.Y., 2013. Forward osmosis treatment of drilling mud and fracturing wastewater from oil and gas operations. *Desalination*, 312, pp.60-66. https://doi.org/10.1016/j.desal.2012.05.037

Jang, A., Jung, J.-T., Kang, H., Kim, H.-S. and Kim, J.-O., 2017. Reuse of effluent discharged from tannery wastewater treatment plants by powdered activated carbon and ultrafiltration combined reverse osmosis system. *Journal of Water Reuse and Desalination*, 7(1), pp.97-102. https://doi.org/10.2166/wrd.2016.001

Kaul, S.N., Nandy, T., Szpyrkowicz, L., Gautam, A. and Khanna, D.R., 2013. Wastewater management with special reference to tanneries (Second Edition). Discovery Publishing House, New Delhi.

Khraisheh, M., Gulied, M. and AlMomani, F., 2020. Effect of membrane fouling on fertilizer-drawn forward osmosis desalination performance. *Membranes*, 10(9), pp.243. https://doi.org/10.3390/membranes10090243

Kim, S.L., Paul Chen, J. and Ting, Y.P., 2002. Study on feed pretreatment for membrane filtration of secondary effluent. *Separation and Purification Technology*, 29(2), pp.171-179. https://doi.org/10.1016/S1383-5866(02)00073-4

Korenak, J., Hélix-Nielsen, C., Bukšek, H. and Petrinić, I., 2019. Efficiency and economic feasibility of forward osmosis in textile wastewater treatment. *Journal of Cleaner Production*, 210, pp.1483-1495. https://doi.org/10.1016/j.jclepro.2018.11.130

Lay, W.C.L., Zhang, J., Tang, C., Wang, R., Liu, Y. and Fane, A.G., 2012. Factors affecting flux performance of forward osmosis systems. *Journal of Membrane Science*, 394–395, pp.151-168. https://doi.org/10.1016/j.memsci.2011.12.035

Li, P., Lim, S.S., Neo, J.G., Ong, R.C., Weber, M., Staudt, C., Widjojo, N., Maletzko, C. and Chung, T.S., 2014. Short and long-term performance of the thin-film composite forward osmosis (TFC-FO) hollow fiber membranes for oily wastewater purification. *Industrial & Engineering Chemistry Research*, 53(36), pp.14056-14064. https://doi.org/10.1021/ie502365p

Li, Z., Valladares Linares, R., Bucs, S., Fortunato, L., Hélix-Nielsen, C., Vrouwenvelder, J.S., Ghaffour, N., Leiknes, T. and Amy, G., 2017. Aquaporin based biomimetic membrane in forward osmosis: Chemical cleaning resistance and practical operation. *Desalination*, 420, pp.208-215. https://doi.org/10.1016/j.desal.2017.07.015

Luo, W., Xie, M., Song, X., Guo, W., Ngo, H.H., Zhou, J.L. and Nghiem, L.D., 2018. Biomimetic aquaporin membranes for osmotic membrane bioreactors: Membrane performance and contaminant removal. *Bioresource Technology*, 249, pp.62-68. https://doi.org/10.1016/j.biortech.2017.09.170

Mondal, M. and De, S., 2015. Characterization and antifouling properties of polyethylene glycol doped PAN–CAP blend membrane. *RSC Advances*, 5(49), pp.38948-38963. https://doi.org/10.1039/C5RA02889B

Morrow, C.P. and Childress, A.E., 2019. Evidence, determination, and implications of membrane-independent limiting flux in forward osmosis systems. *Environmental Science & Technology*, 53(8), pp.4380-4388. https://doi.org/10.1021/acs.est.8b05925

Nguyen, T.A. and Yoshikawa, S., 2019. Modeling and economic optimization of the membrane module for ultrafiltration of protein solution using a genetic algorithm. *Processes*, 8(1), p.4. https://doi.org/10.3390/pr8010004

Omir, A., Satayeva, A., Chinakulova, A., Kamal, A., Kim, J., Inglezakis, V.J. and Arkhangelsky, E., 2020. The behavior of aquaporin forward osmosis flat sheet membranes during the concentration of calcium-containing liquids. *Membranes*, 10(5), p.108. https://doi.org/10.3390/membranes10050108

Ortega-Bravo, J.C., Ruiz-Filippi, G., Donoso-Bravo, A., Reyes-Caniupán, I.E. and Jeison, D., 2016. Forward osmosis: Evaluation of thin-film-composite membrane for municipal sewage concentration. *Chemical Engineering Journal*, 306, pp.531-537. https://doi.org/10.1016/j.cej.2016.07.085

Pal, P., Chakrabortty, S., Nayak, J. and Senapati, S., 2017. A flux-enhancing forward osmosis–nanofiltration integrated treatment system for the tannery wastewater reclamation. *Environmental Science and Pollution Research*, 24(18), pp.15768-15780. https://doi.org/10.1007/s11356-017-9206-z

Panizza, M. and Cerisola, G., 2004. Electrochemical oxidation as a final treatment of synthetic tannery wastewater. *Environmental Science & Technology*, 38(20), pp.5470-5475. https://doi.org/10.1021/es049730n

Pham, M.T., Nishihama, S. and Yoshizuka, K., 2021. Removal of chromium from the water environment by forward osmosis system. *MATEC Web of Conferences*, 333, p.04007. https://doi.org/10.1051/matecconf/202133304007

Pophali, G.R. and Dhodapkar, R.S., 2011. An overview of sustainability of common effluent treatment plant for clusters of tanneries. *Environment, Development and Sustainability*, 13(3), pp.493-506. https://doi.org/10.1007/s10668-010-9272-6

Pramanik, B.K., Roddick, F.A. and Fan, L., 2014. Effect of biologically activated carbon pre-treatment to control organic fouling in the microfiltration of biologically treated secondary effluent. *Water Research*, 63, pp.147-157. https://doi.org/10.1016/j.watres.2014.06.014

Ramteke, P.W., Awasthi, S., Srinath, T. and Joseph, B., 2010. Efficiency assessment of common effluent treatment plant (CETP) treating tannery effluents. *Environmental Monitoring and Assessment*, 169(1–4), pp.125-131. https://doi.org/10.1007/s10661-009-1156-6

Ranganathan, K. and Kabadgi, S.D., 2011. Studies on the feasibility of reverse osmosis (membrane) technology for the treatment of tannery wastewater. *Journal of Environmental Protection*, 02(01), pp.37-46. https://doi.org/10.4236/jep.2011.21004

Roy, D., Rahni, M., Pierre, P. and Yargeau, V., 2016. Forward osmosis for the concentration and reuse of process saline wastewater. *Chemical Engineering Journal*, 287, pp.277-284. https://doi.org/10.1016/j.cej.2015.11.012

Sagiv, A., Zhu, A., Christofides, P.D., Cohen, Y. and Semiat, R., 2014. Analysis of forward osmosis desalination via two-dimensional FEM model. *Journal of Membrane Science*, 464, pp.161-172. https://doi.org/10.1016/j.memsci.2014.04.001

She, Q., Jin, X., Li, Q. and Tang, C.Y., 2012. Relating reverse and forward solute diffusion to membrane fouling in osmotically driven membrane processes. *Water Research*, 46(7), pp.2478-2486. https://doi.org/10.1016/j.watres.2012.02.024

Sundarapandiyan, S., Chandrasekar, R., Ramanaiah, B., Krishnan, S. and Saravanan, P., 2010. Electrochemical oxidation and reuse of tannery saline wastewater. *Journal of Hazardous Materials*, 180(1–3), pp.197-203. https://doi.org/10.1016/j.jhazmat.2010.04.013

Suthanthararajan, R., Ravindranath, E., Chits, K., Umamaheswari, B., Ramesh, T. and Rajamam, S., 2004. Membrane application for recovery and reuse of water from treated tannery wastewater. *Desalination*, 164(2), pp.151-156. https://doi.org/10.1016/S0011-9164(04)00174-2

Sweity, A., Oren, Y., Ronen, Z. and Herzberg, M., 2013. The influence of antiscalants on biofouling of RO membranes in seawater desalination. *Water Research*, 47(10), pp.3389-3398. https://doi.org/10.1016/j.watres.2013.03.042

Tasci, R. O., Kaya, M. A. and Celebi, M., 2022. Hydrophilicity and flux properties improvement of high-performance polysulfone membranes via sulfonation and blending with Poly(lactic acid). *High-Performance Polymers*, 34(10), pp. 1115–1130. https://doi.org/10.1177/09540083221110031

Thiruvenkatachari, R., Francis, M., Cunnington, M. and Su, S., 2016. Application of integrated forward and reverse osmosis for coal mine wastewater desalination. *Separation and Purification Technology*, 163, pp. 181–188. https://doi.org/10.1016/j.seppur.2016.02.034

Vital, B., Bartacek, J., Ortega-Bravo, J. C. and Jeison, D., 2018. Treatment of acid mine drainage by forward osmosis: Heavy metal rejection and reverse flux of draw solution constituents. *Chemical Engineering Journal*, 332, pp. 85–91. https://doi.org/10.1016/j.cej.2017.09.034

Zaviska, F., Chun, Y., Heran, M. and Zou, L., 2015. Using FO as pre-treatment of RO for high scaling potential brackish water: Energy and performance optimization. *Journal of Membrane Science*, 492, pp. 430–438. https://doi.org/10.1016/j.memsci.2015.06.004

Zhao, J., Wu, Q., Tang, Y., Zhou, J. and Guo, H., 2022. Tannery wastewater treatment: Conventional and promising processes, an updated 20-year review. *Journal of Leather Science and Engineering*, 4(1), pp. 10. https://doi.org/10.1186/s42825-022-00082-7